Hindawi Publishing Corporation
Journal of Robotics
Volume 2013, Article ID 535106, 20 pages
http://dx.doi.org/10.1155/2013/535106

Research Article

Design and Evaluation of the AIRGAIT Exoskeleton: Leg Orthosis Control for Assistive Gait Rehabilitation

Mohd Azuwan Mat Dzahir[1,2] and Shin-Ichiroh Yamamoto[1]

[1] *Shibaura Institute of Technology, Department of Bio-Science Engineering, 307 Fukasaku, Minuma-ku, Saitama City, Saitama 337-8570, Japan*
[2] *Universiti Teknologi Malaysia, Faculty of Mechanical Engineering, 81310 UTM Skudai, Johor Bahru, Malaysia*

Correspondence should be addressed to Mohd Azuwan Mat Dzahir; azuwan@fkm.utm.my

Received 18 July 2013; Accepted 21 September 2013

Academic Editor: Kazuhiko Terashima

This paper introduces the body weight support gait training system known as the AIRGAIT exoskeleton and delves into the design and evaluation of its leg orthosis control algorithm. The implementation of the mono- and biarticular pneumatic muscle actuators (PMAs) as the actuation system was initiated to generate more power and precisely control the leg orthosis. This research proposes a simple paradigm for controlling the mono- and bi-articular actuator movements cocontractively by introducing a cocontraction model. Three tests were performed. The first test involved control of the orthosis with monoarticular actuators alone without a subject (WO/S); the second involved control of the orthosis with mono- and bi-articular actuators tested WO/S; and the third test involved control of the orthosis with mono- and bi-articular actuators tested with a subject (W/S). Full body weight support (BWS) was implemented in this study during the test W/S as the load supported by the orthosis was at its maximum capacity. This assessment will optimize the control system strategy so that the system operates to its full capacity. The results revealed that the proposed control strategy was able to co-contractively actuate the mono- and bi-articular actuators simultaneously and increase stiffness at both hip and knee joints.

1. Introduction

Considerable assistive gait rehabilitation training methods for the neurologically impaired (including stroke and spinal cord injury (SCI) patients) have been developed using a variety of actuation systems to generate the necessary force to operate the leg orthosis. One of the best examples of gait rehabilitation orthosis is the LOKOMAT (Hocoma AG, Volketswill, Switzerland) or driven gait orthosis (DGO) which is commercially available and extensively researched in many rehabilitation centres [1–3]. This orthosis uses a DC motor for the actuation power to control trajectory at the hip and knee joints. Initially, this DGO implemented the position controller for the control system. However, with further research, this method was improved with the addition of the adaptive and impedance controllers. Emphasis is placed on providing adequate afferent input to stimulate the locomotor function of the spinal cord and activate leg muscles that have lost the capacity to actuate voluntary movement. On the other hand, The Lower Extremity Powered Exoskeleton (LOPES) is a gait rehabilitation orthosis that employs the Bowden-cable driven series elastic actuator (SEA) with the servo-motors as the actuation system to implement low-weight (pure) force sources [4, 5]. This orthosis uses impedance control as opposed to admittance control and is based on position sensing combined with force actuation to operate the lower limb extremity orthosis. This orthosis emphasises on incorporating the Assist as Needed (AAN) algorithm into the system to enhance the training effect by increasing the active participation of patients.

Conversely, robot-assisted gait training (RAGT) with an active leg exoskeleton (ALEX) implemented linear actuators to manipulate the thigh device (hip joint) and shank device (knee joint) [6, 7]. This exoskeleton uses a force-field controller by effectively applying forces on the ankle of the subject through actuators located at the hip and knee joints. They

also incorporate the AAN paradigm for rehabilitation into the system which allows patients to participate more actively in the retraining process compared to other currently available robotic training methods. There is also a neurorehabilitative platform for bedridden poststroke patients (NEUROBike) that employs the use of brushless servomotors and pulleys to actively control the angular excursions of the gait orthosis [8]. This system implements the kinematic models of leg-joint angular excursions during both walking and "sit-to-stand" into the control algorithms to carry out passive and active exercises. The aim of this system is to provide several exercises at an early stage according to the severity of the pathology and the intensity required by the programmed therapy.

The pneumatically operated gait orthosis (POGO) which utilizes pneumatic cylinders as an actuation system is another development [9]. This system incorporated the force and position controller to conform to the pelvis and legs of the subject to desired patterns. Due to the importance of generating normal sensory input during gait training, the POGO developed a device that can accommodate and control the naturalistic motion of the pelvis. In contrast, the robotic gait rehabilitation (RGR) trainer uses servotube linear electromagnetic actuators to generate the power source for the exoskeleton [10]. This system uses an expanded impedance control strategy by switching the force field that affects the obliquity of the pelvis to generate the corrective moments only when the leg is in swing motion. This system was based on the hypothesis that correction of a stiff-legged gait pattern requires addressing both the primary and secondary gait deviations to restore a physiological gait pattern. A newly developed gait training robotic device is LOKOIRAN which employs AC motors connected to a slide-crank mechanism via belts and pulleys to provide the energy for the system [11]. This system engages the speed control mode and the admittance control mode to manage trajectory of the joints in the robotic device. The objective of this system is to develop a passive orthosis to fully support the patient and provide joint angle data during training.

Recently, a robotic orthosis for gait rehabilitation utilising PMAs was developed [12, 13]. This system incorporated the AAN gait training algorithm based on the adaptive impedance control which uses a boundary-layer-augmented sliding mode control- (BASMC-) based position controller to provide interactive robotic gait training. However, it only implemented the use of monoarticular actuators at the hip and knee joints to actuate the leg orthosis without considering the implementation and control of bi-articular actuators. Previous research on the AIRGAIT exoskeleton suggests that the cocontraction of pneumatic McKibben actuators which set up an antagonistic arrangement of bi-articular muscles is able to increase stiffness of both hip and knee joints of the orthosis [14, 15]. However, these antagonistic bi-articular actuators only exerted a constant input pressure of 2.5 (bars) alternately at both sides. In view of this, this research introduces the designed controller scheme and strategy to optimize the control of bi-articular actuators and actuate them in co-contractive-like movements. The approach strategy for this designed controller scheme is the derivation of a cocontraction model which facilitates the implementation of position and pressure-based controllers which manage the antagonistic mono- and bi-articular actuators simultaneously. To the authors' best knowledge, assistive leg orthosis that emphasizes on the control of antagonistic bi-articular actuators using the PMA in the gait rehabilitation field is yet to be extensively investigated and made commercially available. This then provides the motivation and purpose for this research.

2. Design System of AIRGAIT Exoskeleton

Figure 1 shows the schematic diagram for the AIRGAIT exoskeleton. The design of this system and the mechanical structures involved were thoroughly evaluated in previously published papers [14, 15]. Currently, the AIRGAIT exoskeleton employs the PC-based control which utilizes the xPC-Target toolbox and MATLAB/Simulink software as the operating system. The input data is generated within the host-PC and then transferred to the target-PC using the D/A converter to operate the electropneumatic regulators. To realize the cocontraction movements between the antagonistic mono- and bi-articular actuators, one regulator for each actuator was used. Then, measurements by the system (i.e., joints' angle and PMAs' pressure) provide feedback to the host-PC through the A/D converter. The rotary potentiometer (contactless Hall-IC angle sensor CP-20H series, MIDORI PRECISIONS) was used to determine the trajectory of the hip and knee joints and then manage the PMAs' contraction parameters using a position controller. The compact pressure sensor for pneumatic actuators (PSE540-R06, SMC) was used to read the pressure level in each PMA, and the input patterns of the PMAs were managed with the utilisation of a pressure controller. This system will be converted to the Lab-View system for the implementation of real-time control of gait rehabilitation.

2.1. Mechanical Structure of the Leg Orthosis. The structure of the leg orthosis covers the thigh at the lower end of hip joint and shank at the lower end of the knee joint. The ankle joint orthosis was not included as the foot clearance during swing can be realized by implementing elastic straps, a passive foot lifter, or passive orthosis [1, 4]. However, for the implementation of the passive orthosis, the research on the ankle orthosis of the AIRGAIT exoskeleton was conducted separately. This leg orthosis was fixed in a sagittal plane at the pelvis rotation to facilitate gait motion training for the hip and knee joints [1, 4, 6, 10, 12]. The sagittal plane is a vertical plane which passes from ventral (front) to dorsal (rear) dividing the body into the right and left halves as shown in Figure 1(b). Weight compensation for leg orthosis is provided for by the parallel linkage and gas spring mechanisms. This limits vertical motion during the training session [1, 4, 6, 10, 12]. The upper and lower parts of the leg orthosis (i.e., thigh and shank) can be adjusted to agree with the height of the subject. Parallel bars were used to attach the end connectors of the mono- and bi-articular actuators (PMAs) at the anterior and posterior sides of the leg orthosis. By using the slider, these parallel bars can be adjusted accordingly to maximise the outcome of the joints angle trajectory.

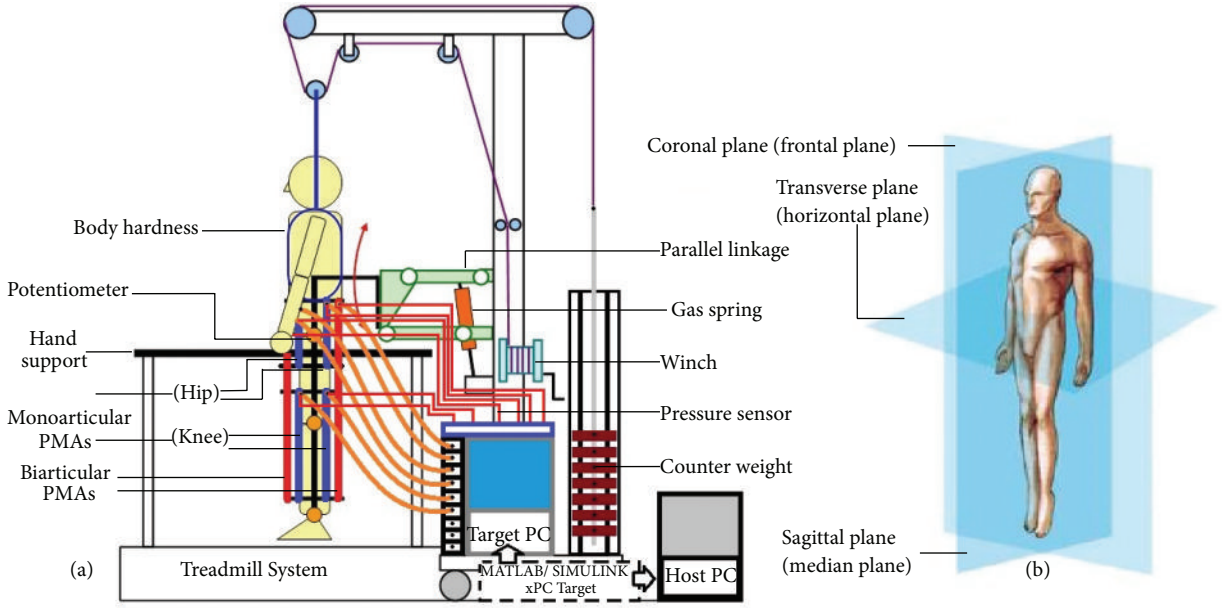

Figure 1: Schematic diagram for body weight support gait training system (AIRGAIT).

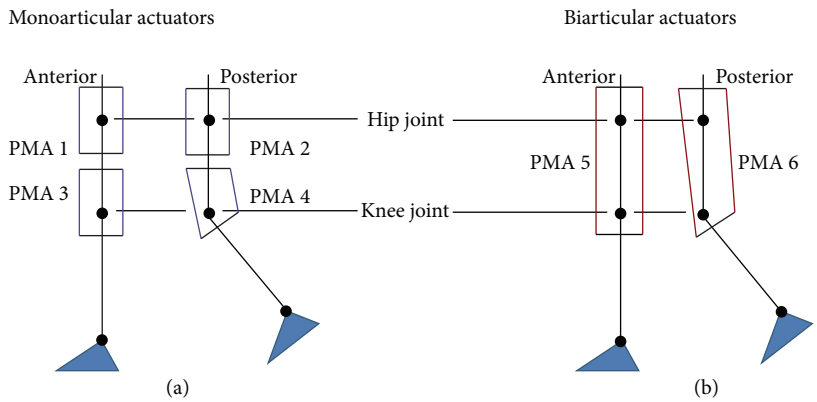

Figure 2: PMAs' setting; (a) antagonistic mono-articular (hip and knee joints) actuators and (b) bi-articular actuators.

2.2. Mono- and Biarticular Muscle Actuators. The implementation of mono- and bi-articular actuators to actuate the AIRGAIT exoskeleton leg orthosis is based on the McKibben muscle actuator. These actuators were fabricated within our laboratory using special tools which were designed to assemble the parts of the actuator (i.e., rubber tube, braided fabric, copper ring, end connector, and input connector). The implementation of these mono- and bi-articular actuators is based on the various human muscles (i.e., gluteus maximus, gluteus minimus, gluteus medius, vastus lateralis, gastrocnemius, rectus femoris, and hamstring) and antagonistically (i.e., anterior and posterior) attached to the leg orthosis. Compared to monoarticular actuators, bi-articular actuators require accurate input patterns to simultaneously actuate the antagonistic actuators which control two joint angles [14, 15]. Although the bi-articular actuators may be considered redundant in the actuation system, the strong force they generate will improve the maximum angle extension, provide precise movements, and ensure balance between antagonistic actuators and stiffness at the joints [16–20].

The position setting of the antagonistic actuators is illustrated in the Figure 2, where the position of the antagonistic mono-articular actuators both for the hip and knee joints is placed in between the antagonistic bi-articular actuators. This then provides the antagonistic bi-articular actuators with an extra length which helps in achieving much wider movement at the joints. The details on the best setup determination of the antagonistic actuators were recorded earlier and can be referred to in [21].

2.3. AIRGAIT Prototype. The prototype of the AIRGAIT exoskeleton was developed in 2010 and extensively researched for improvement. However, it is yet to be commercialized. The research on gait training is progressing rapidly towards enhancement in design structures and control algorithms. A lone operator is sufficient for the running of this system. The

(a) (b)

Figure 3: Body weight support gait training system (AIRGAIT) prototype.

process involves providing the subject with information on the training procedures and experiment protocols, putting on of the body harness, attaching the assisted leg orthosis to the lower limb of the subject, and finally, proceeding with the gait training or experiment. Figure 3 shows the prototype of the AIRGAIT exoskeleton.

2.4. Mechanical System. The mechanical structure of the AIRGAIT exoskeleton is made up of three main parts which are (a) the BWS system which consists of the body harness and counter weight, (b) the treadmill training which involves the treadmill and hand support, and (c) the assistive gait training which comprises the lower limb powered orthosis, spring, and parallel linkage (parallelogram). The spring and parallel linkage were fixed in a sagittal plane so that the gait motion training at hip and knee joints can be realized. The sagittal plane also compensates for the vertical weight load from the system [1, 4, 10, 12]. The subject is provided with the BWS so that he/she will be able to maintain his/her balance during the gait training or experimental tests [11, 22, 23]. A variable speed treadmill is also provided for the assisted leg orthosis gait training and the body weight support gait training [23, 24].

2.5. Safety Features. To ensure the safety of the subject during the assisted gait rehabilitation and experimental tests, several safety features were included in the AIRGAIT exoskeleton design. The implementation of the PMA as the actuation system is in itself a safety feature due to its naturally compliant mechanism [25]. Also, the exclusion of the possibility of short circuits in the actuation system during operation makes it suitable for the human-robot interaction. Moreover, as the system involves compressed air and the expansion and contraction of the braided rubber tube, it is possible to perform the orthosis in an underwater rehabilitation training scenario. Our earlier laboratory study of the robotic gait trainer (RGTW) indicated that hydrotherapy may be particularly effective in the treatment of individuals with hip joint movement dysfunction [26]. Since the PMA characteristics are based on its model parameters such as dimension (i.e., length and contraction) and pressure, the maximum contraction of PMA will prevent the exoskeleton of the AIRGAIT leg orthosis from exceeding the limitation of the joints [27]. However, as a further precaution, a stopper was positioned at the hip and knee joints of the leg orthosis to avoid the unexpected and provide another safety feature. Additionally, the implementation of the BWS system ensures that the subject is able to maintain his/her balance and not fall over while on the treadmill [22, 23].

3. Materials and Methods

3.1. Procedures. The exoskeleton of the AIRGAIT leg orthosis is first adjusted to correspond with the position of the hip and knee joints of the subject to obtain precise data during the experimental tests. Then, the controller parameters for the antagonistic mono-articular actuators (i.e., hip and knee joints) are tuned until good joint trajectory is attained. This is followed by the tuning of antagonistic bi-articular actuator controller parameters. The control for the leg orthosis WO/S is then set for different gait cycle (GC) speeds, and data for the trajectory of the hip and knee joints are gathered. The steps taken for testing W/S are (a) the subject is provided with sufficient information regarding the tests and procedures, (b) the subject is fitted with a body harness and a passive foot lifter was secured at the ankle joint before the leg orthosis was attached to the subject, and (c) the subject is provided with the full BWS before the control of leg orthosis was performed at different GC speeds including that of an average human. Table 1 below shows the existing lower limb gait rehabilitation orthosis systems such as LOKOMAT, LOPES, ALEX, Robotic Orthosis for Gait Rehabilitation, and our research AIRGAIT in terms of (1) type of actuator used as the actuation system; (2) number of joint manipulators; (3) plane of actuated DOFs; and (4) GC operating speed.

3.2. Experimental Tests. Three tests were conducted for the experimental study. These tests were performed on one side of the exoskeleton of the AIRGAIT leg orthosis. The first test was conducted using two sets of antagonistic mono-articular

Table 1: Existing lower limb gait rehabilitation orthosis systems comparison.

Comparison between existing lower limb gait rehabilitation orthosis systems					
Orthosis system	Type of actuator	Number of joints	Actuated DOFs	Operating speed	References
LOKOMAT	DC motors	Hip and knee joints, passive foot lifter was applied at ankle Joint	Sagittal plane	0.56 m/s	[1–3]
Lower Extremity Powered Exoskeleton (LOPES)	Bowden cable series elastic actuators (SEA) and servomotors	Hip and knee joints, elastic straps was applied at ankle joint	Sagittal plane	0.75 m/s	[4, 5]
Active Leg Exoskeleton (ALEX)	Linear actuators	Hip, knee, and ankle joints	Sagittal plane	0.40 m/s up to 0.85 m/s	[6, 7]
Robotic Orthosis for Gait Rehabilitation	Pneumatic muscle actuators (monoarticular actuators)	Hip and knee joints, foot lifter was used at ankle joint	Sagittal plane	0.60 m/s	[12, 13]
Body Weight Support Gait Training System (AIRGAIT)	Pneumatic muscle actuators (mono- and biarticular actuators)	Hip and knee joints, foot lifter was used at ankle joint	Sagittal plane	0.35 m/s (4s GC), 0.47 m/s (3s GC), 0.70 m/s (2s GC), and 1.40 m/s (1s GC)	

actuators (i.e., hip and knee joints) tested WO/S; the second with the addition of one set of antagonistic bi-articular actuators tested WO/S; and the third with the addition of one set of antagonistic bi-articular actuators tested W/S. Full BWS was implemented in this study during the test W/S as the load supported by the orthosis was at its maximum capacity. This assessment will optimize the control system strategy so that it operates at its maximum capability. The options for the subject were not really critical as the focus of the research is on the design controller. As such, the subject chosen was young, healthy, and not bearing any neurological disorder. With this, we were able to instruct the subject to be passive during the experimental tests. To achieve the natural posture of gait motion during training, the passive foot lifter was used to ensure enough foot clearance during the swing phase [1, 4].

The control of the leg orthosis WO/S and W/S is displayed in Figures 4 and 5. For the first and second tests (WO/S), GC speeds of 4 seconds, 3 seconds, 2 seconds, and 1 second were evaluated for the design controller scheme. Four GC speeds were also evaluated for the third test (W/S). Five trials were performed for each GC speed, and each trial consisted of five cycles including the initial cycle position. The total GCs performed for each GC speed was around 25 cycles. The average GC was then calculated and represented in a graph. Based on these data, three comparative evaluations were analysed to determine the design controller scheme and strategy performance. These were (a) between the mono-articular actuators alone (i.e., hip and knee joints) and with bi-articular actuators, (b) between the cocontraction model based position (P) controller scheme and the cocontraction model based position-pressure (PP) controller scheme tested WO/S, and (c) between the cocontraction model based P controller scheme and the cocontraction model based PP controller scheme tested W/S. The design controller scheme and strategy performance were evaluated based on the GC, movement of hip and knee joints trajectory, maximum joint angle extension, inertia, gravitational effect, and time shift.

4. Control System

4.1. Controller Algorithm. Figure 6 shows the schematic diagram of the exoskeleton of the AIRGAIT leg orthosis controller schemes. Figure 6(a) shows the cocontraction model based P controller, and Figure 6(b) shows the cocontraction model based PP controller. Unlike other control algorithms for PMA, the designed controller scheme does not predict or measure the required torque at the joints [25, 28–30]. Rather, it correlates the angle information of the joints with the dynamic characteristics of the PMA (i.e., contraction and pressure) and then realizes the position and pressure controls. In order to implement this controller scheme, the cocontraction model was developed. The control strategy was to execute the cocontraction model based position-pressure controller scheme. The position controller was used to tune the cocontraction model parameters (activation levels) while the pressure controller was used to control the input patterns of the antagonistic mono- and bi-articular actuators. The derived cocontraction model provides the input patterns for the mono- and bi-articular actuators and simultaneously actuates the antagonistic actuators cocontractively, while the PMA model was determined in order to consider the characteristics of the PMA that were to be introduced into the controller design. This dynamic model was evaluated in an experimental study and represented in an equation. The proposed controller scheme was specifically designed for simplifying the control of antagonistic bi-articular actuators so as to enhance the stiffness at both hip and knee joints. It is an arduous task to construct the plant model of leg orthosis (with antagonistic mono- and bi-articular PMAs) for the implementation of the Stochastic Optimization method to determine the control parameters of the design controller. As such, the heuristic method was implemented.

4.2. Cocontraction Model. The cocontraction model generates the input patterns for the antagonistic mono- and

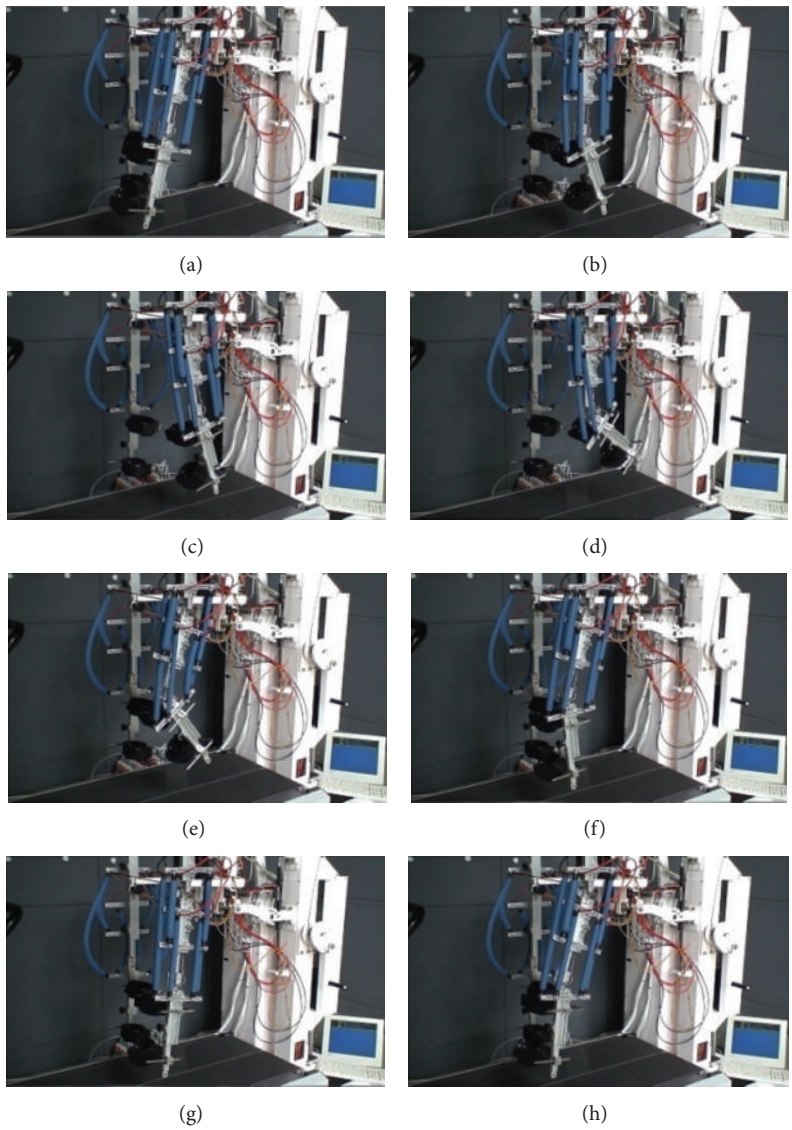

Figure 4: Control of the leg orthosis without a subject (WO/S).

bi-articular actuators (i.e., anterior and posterior) in order to realize the method for implementing the position-pressure controller scheme. This model correlates information on the joints with the dynamic characteristics of the PMA (i.e., contraction and pressure). Based on the derived mathematical model, the contraction of antagonistic mono-articular actuators can be characterized as proportional and inversely proportional (1st-order system) to the angle of the joint. As for the bi-articular actuators, a much higher-order system is required to enable these actuators to manage two joints simultaneously. To control these joints effectively, the input patterns for the antagonistic bi-articular actuators should be sufficiently accurate as this will ensure the efficient performance of the antagonistic mono-articular actuators and facilitate co-contractive movements between the antagonistic actuators. Determination of the co-contractive input for the bi-articular actuators is insufficient to achieve complete gait motion of the leg orthosis without the inclusion of mono-articular actuators. Thus, the role played by the control of the mono-articular actuators is crucial in the successful implementation of the bi-articular actuators.

Figure 7 shows the process of measuring the reference signal (input patterns) for the antagonistic mono- and bi-articular actuators. Figure 7(a) shows the reference angle of hip and knee joints. Point (A) shows the maximum contraction input pattern for the anterior actuators and minimum contraction input pattern for the posterior actuators as shown in Figure 7(b). Point (B) shows the maximum contraction input pattern for the posterior actuators and minimum contraction input pattern for the anterior actuators as shown in Figure 7(c). Based on this positional data information, the contraction patterns (i.e., $C1$–$C6$) of the mono- and bi-articular actuators were then determined using the mathematical derivation as follows.

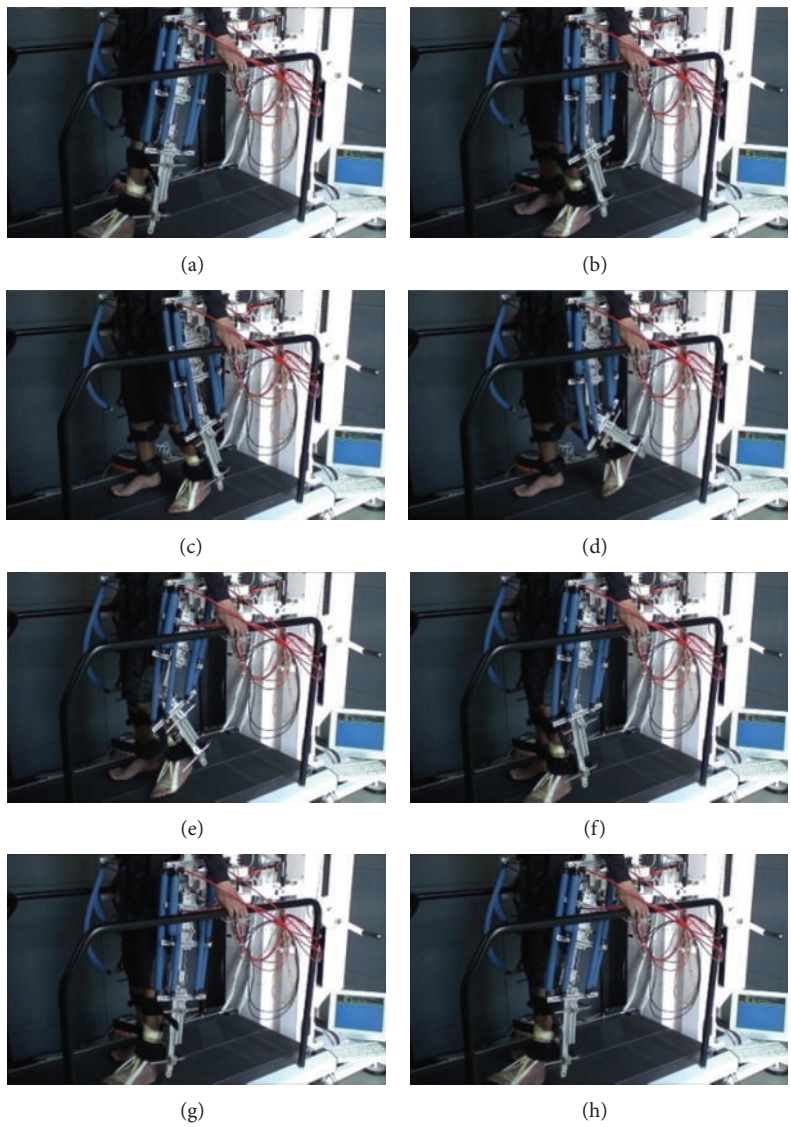

(a) (b) (c) (d) (e) (f) (g) (h)

Figure 5: Control of the leg orthosis with a subject (W/S).

Mono-articular actuators for the hip joint:

$$C1 = \varepsilon_{ha}(t) = \left(\frac{r_h}{l_{o_{\text{hip}}}}\right) \cdot \alpha_h \cdot \theta_{ha}(t) \leq 0.3,$$
$$C2 = \varepsilon_{hp}(t) = \left(\frac{r_h}{l_{o_{\text{hip}}}}\right) \cdot \beta_h \cdot \theta_{hp}(t) \leq 0.3. \quad (1)$$

Mono-articular actuators for the knee joint:

$$C3 = \varepsilon_{ka}(t) = \left(\frac{r_k}{l_{o_{\text{knee}}}}\right) \cdot \alpha_k \cdot \theta_{ka}(t) \leq 0.3,$$
$$C4 = \varepsilon_{kp}(t) = \left(\frac{r_k}{l_{o_{\text{knee}}}}\right) \cdot \beta_k \cdot \theta_{kp}(t) \leq 0.3. \quad (2)$$

Bi-articular actuators for hip and knee joints:

$$C5 = \varepsilon_{ba}(t) = \left(\frac{r_{\text{bi}}}{l_{o_{\text{bi}}}}\right) \cdot \alpha_{\text{bi}} \cdot \left(\theta_h(t) + \theta_k(t)\right)_a \leq 0.3,$$
$$C6 = \varepsilon_{bp}(t) = \left(\frac{r_{\text{bi}}}{l_{o_{\text{bi}}}}\right) \cdot \beta_{\text{bi}} \cdot \left(\theta_h(t) + \theta_k(t)\right)_p \leq 0.3, \quad (3)$$

where ε is the contraction patterns; r is the PMAs distance from the joints; l_o is the PMA initial length; α and β are the anterior and posterior muscle activation levels; and 0.3 value is the PMAs' maximum contraction. The derivation of this cocontraction model for the mono- and bi-articular actuators was recorded earlier and can be referred to in [31].

This model was first verified by using the least squares (LS) and recursive least squares (RLS) prediction methods between the inputs patterns and the joint angles as can be seen in Table 2. The coding was programmed in MATLAB

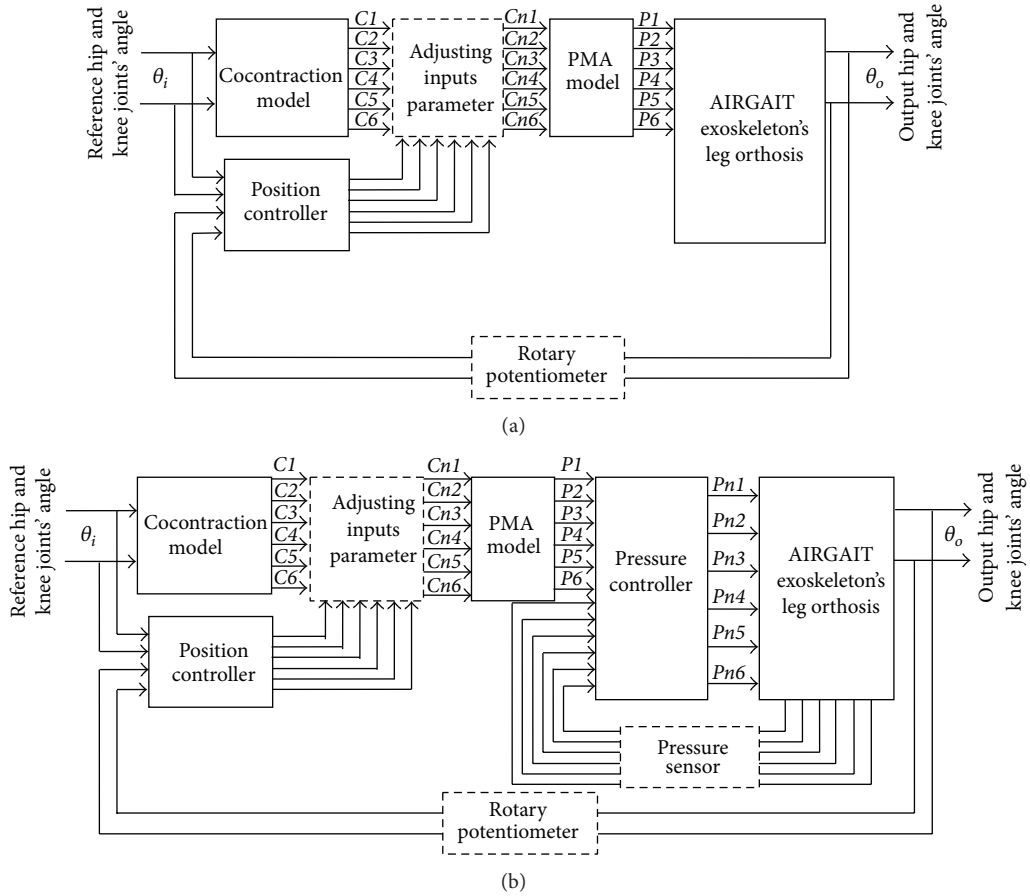

Figure 6: Schematic diagram of the exoskeleton of the AIRGAIT leg orthosis controller schemes. (a) Cocontraction model based P controller and (b) cocontraction model based PP controller, where ($C1$–$C6$) are the contraction input patterns, ($Cn1$–$Cn6$) are the corrected contraction input patterns, ($P1$–$P6$) are the pressure input patterns, and ($Pn1$–$Pn6$) are the corrected pressure input patterns.

Table 2: Input patterns model verification using LS and RLS prediction methods.

PMA actuators	LS and RLS prediction between the input patterns and the joint angles			
	LS method		RLS method	
	1st order	nth order	1st order	nth order
Monoarticular (hip)-Anterior PMA	Yes (proportional)	—	Yes (proportional)	—
Monoarticular (hip)-Posterior PMA	Yes (inversely proportional)	—	Yes (inversely proportional)	—
Monoarticular (knee)-Anterior PMA	Yes (proportional)	—	Yes (proportional)	—
Monoarticular (knee)-Posterior PMA	Yes (inversely proportional)	—	Yes (inversely proportional)	—
Biarticular (hip)-Anterior PMA	No	No	No	No
Biarticular (hip)-Posterior PMA	No	No	No	No

language. Based on the predetermine Transfer Function (TF), the contraction of antagonistic mono-articular actuators can be differentiated as proportional and inversely proportional (1st-order system) to the angle of the joint. However, the model for the antagonistic bi-articular actuators cannot be verified by using the LS and RLS prediction methods, as it requires much higher-order and complex system. This could be verified by using nonlinear ARX model or genetic algorithm (GA).

4.3. PMA Model. The development of the PMA model is for the purpose of increasing the effectiveness of the cocontraction model. While the cocontraction model provides the antagonistic actuators with the contractive data, this model translated that data into pressure patterns [in Volts] for activating the electropneumatic regulators. The dynamic characteristics of the PMA such as dimension (i.e., length and muscle contraction), pressure, and force data were determined in an experimental study. A model equation was

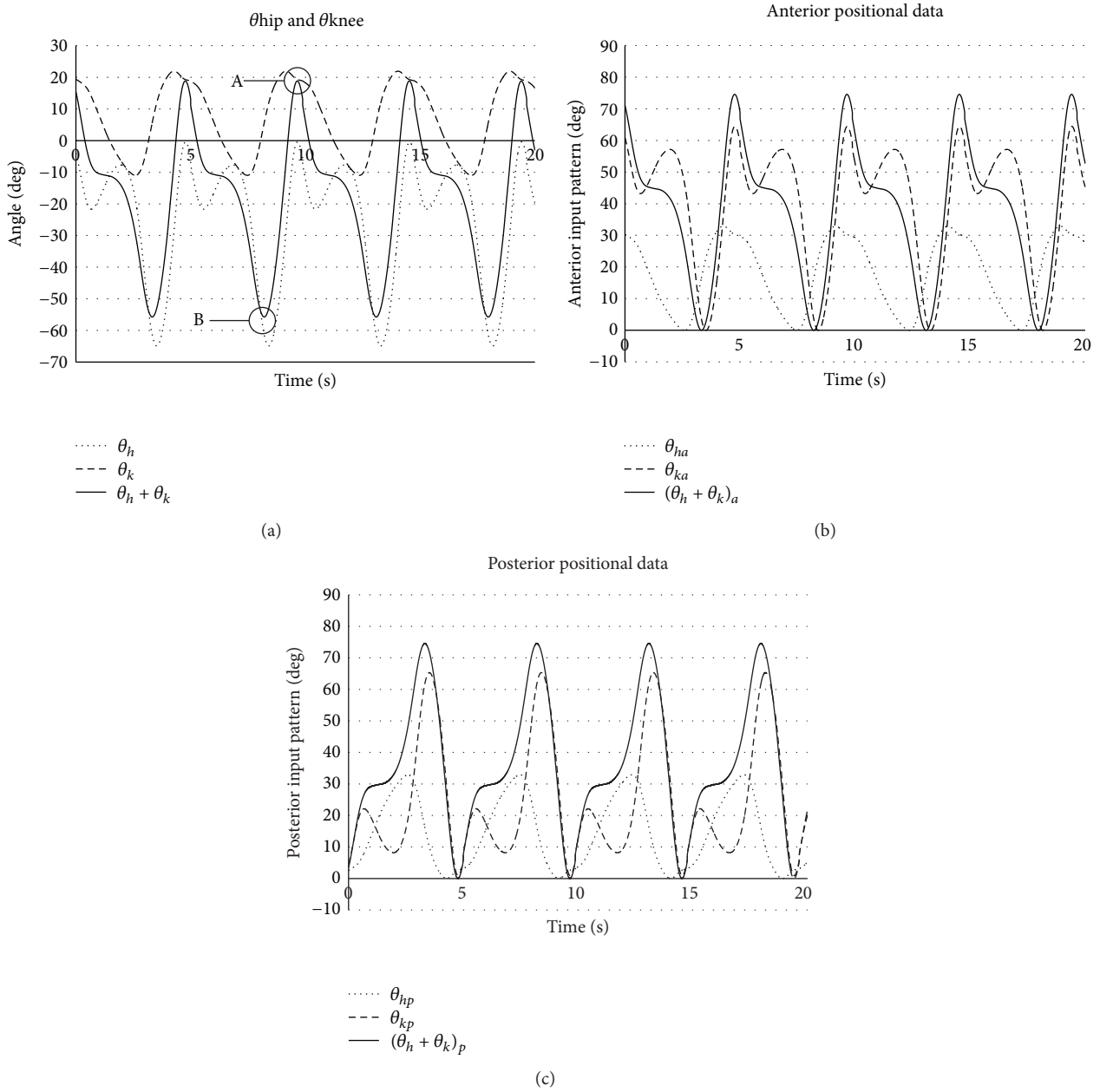

FIGURE 7: Input patterns of the antagonistic mono- and bi-articular actuators. θ_h is the hip joint angle; θ_k is the knee joint angle; θ_{ha}, θ_{ka}, and $(\theta_h + \theta_k)_a$ are the positional data for the anterior actuators; and θ_{hp}, θ_{kp}, and $(\theta_h + \theta_k)_p$ are the positional data for the posterior actuators.

then formulated to represent the PMA characteristics data with the high accuracy of 6th-order polynomial. This will be used as the reference model for the control strategy as can be seen in Figure 8. The cocontraction model control scheme considers the nonlinearity behaviour of the PMA by controlling the muscle activation level of the PMA. The PMA static model at zero load condition was defined as the minimum boundary to determine the nonlinearity area of the PMA. As the critical muscle activity with regard to the PMA is during its contraction, only the contraction mode was considered to realize the cocontraction movements between the antagonistic mono- and bi-articular actuators. The evaluation and derivation of this PMA model have been recorded earlier and can be observed in [21].

5. Results and Discussion

In this section, findings for the designed controller scheme tests and strategy were evaluated and discussed. The modus operandi from the early stage until the final stage was appropriately modelled to optimize the flow of this research. The discussion and evaluation of the findings were divided into three parts to explain each stage of the study. It comprises three assessments for evaluating the performance of the

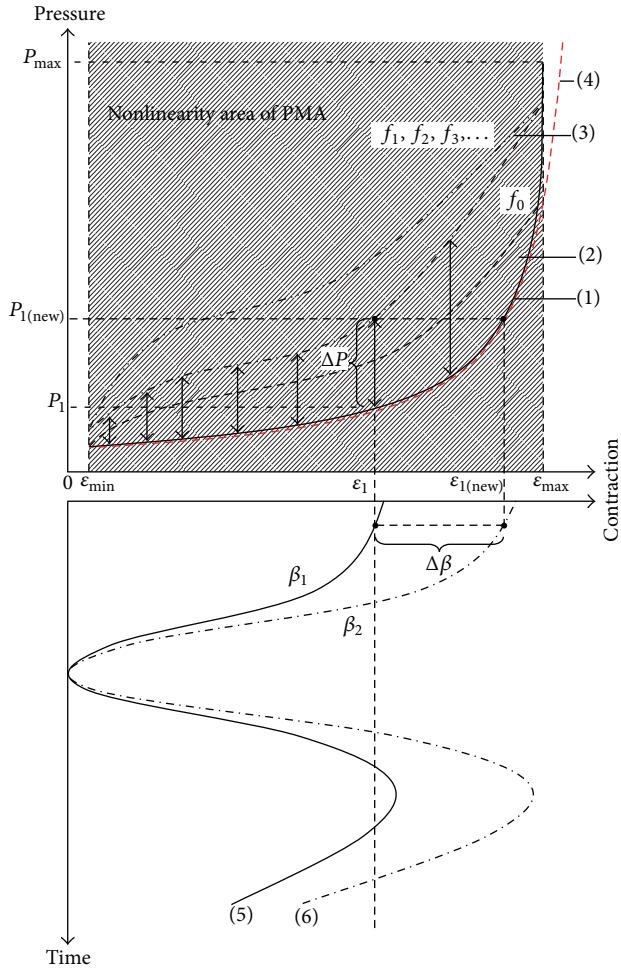

Figure 8: Cocontraction model control scheme's strategy, where (1) PMA static model of pressure versus contraction at zero load condition; (2) PMA hysteresis model at zero load (f_0) condition; (3) PMA hysteresis model at load ($f_1, f_2, f_3, \ldots$) condition; (4) PMA model using 6th-order polynomial equation; (5) contraction input pattern for the antagonistic mono- and bi-articular actuators; (6) controlled contraction input patterns after the controls of the muscle activation level (β); ΔP is the sudden increase in pressure due to the PMA nonlinearity; and $\Delta\beta$ is the increase in muscle activation level.

design controller scheme. These assessments are (a) comparison between the mono-articular actuators acting on their own (i.e., hip and knee joints) and with the addition of bi-articular actuators, (b) comparison between the cocontraction model based position (P) controller and the cocontraction model based position-pressure (PP) controller, and (c) comparison between the control of the leg orthosis WO/S and control of the leg orthosis W/S. The evaluation was based on the GC, movement of the trajectory of the hip and knee joints, maximum angle extension of the joints, inertia, gravitational effect, and time shift.

5.1. Control of the Leg Orthosis WO/S: Evaluation on Antagonistic Actuators. The focus of this assessment is on the implementation of cocontraction input patterns to control the mono- and bi-articular actuators of the exoskeleton of the AIRGAIT leg orthosis. It was conducted to determine the limitations when using mono-articular actuators alone and the advantages to be gained with the inclusion of bi-articular actuators. Two tests were conducted. The first using the mono-articular actuators only (i.e., hip and knee joints) tested WO/S and the second with the addition of bi-articular actuators tested WO/S. These tests were evaluated at four GC speeds of 4 seconds, 3 seconds, 2 seconds, and 1 second so as to raise the stakes of the design controller and the appraisal of the strategy by increasing the GC speed. A total of 25 GCs were performed for each GC speed including the initial position cycle, and data related to the trajectory of the joints were then gathered. The average GC for each GC speed was measured and represented in a graph.

Figures 9 and 10 show the trajectory evaluation of the joints of the leg orthosis controls between two settings (i.e., mono-articular actuators only and with the inclusion of bi-articular actuators) tested WO/S using a cocontraction model based PP controller. Based on the four GC speeds evaluation, it is evident that the leg orthosis was able to perform the gait motion smoothly up to a GC speed of 2 seconds. For the GC speeds of 4 seconds, 3 seconds, and 2 seconds, the orthosis displayed the complete gait motion (i.e., heel strike, foot flat, middle swing, and wide swing) by implementing the designed controller scheme. With the increments in GC speed, the time allocated for completing one GC will be reduced as the graph shifted forward. However, even with the forward shifting of the graph, the time delay in the system was only approximately 0.2 seconds for each GC speed. For the control of leg orthosis using mono-articular actuators alone, it was expected that the trajectory of the joints will be slightly coarse due to the nonlinearity behaviour (i.e., compressible and hysteresis) of the PMA. Although this result may suggest that mono-articular actuators alone are able to support the orthosis, it must be noted that this evaluation was conducted WO/S. The situation changes during implementation W/S as the weight attributed to the actuators is increased. When the inertia and gravitational effect are included in the equation, the limitations of mono-articular actuators acting alone become evident as each actuator is only capable of sustaining a pressure level of 5 (bars). Moreover, due to the position of the antagonistic actuators, the length of mono-articular actuators is much shorter than those of bi-articular actuators. This reduces the maximum angle extension the joints can achieve especially at the knee where a much wider movement (63 degrees) is required compared to the hip. This maximum angle extension is the maximum value of reference angle of the hip and knee joints, both the anterior and posterior sides. This value can be inferred from Winter [32].

However, with the introduction of the bi-articular actuators, the coarse movement was reduced and the stiffness at the joints was improved due to the significant force exerted by these actuators. Manipulators that, equipped with bi-articular actuators have been proved to have numerous advantages such as (1) dramatically increase in range of end effectors, (2) improvement of balance control, (3) efficiency increase of output force production, and (4) an arm that is equipped with bi-articular actuators having the ability to produce a maximum output force at the end effectors

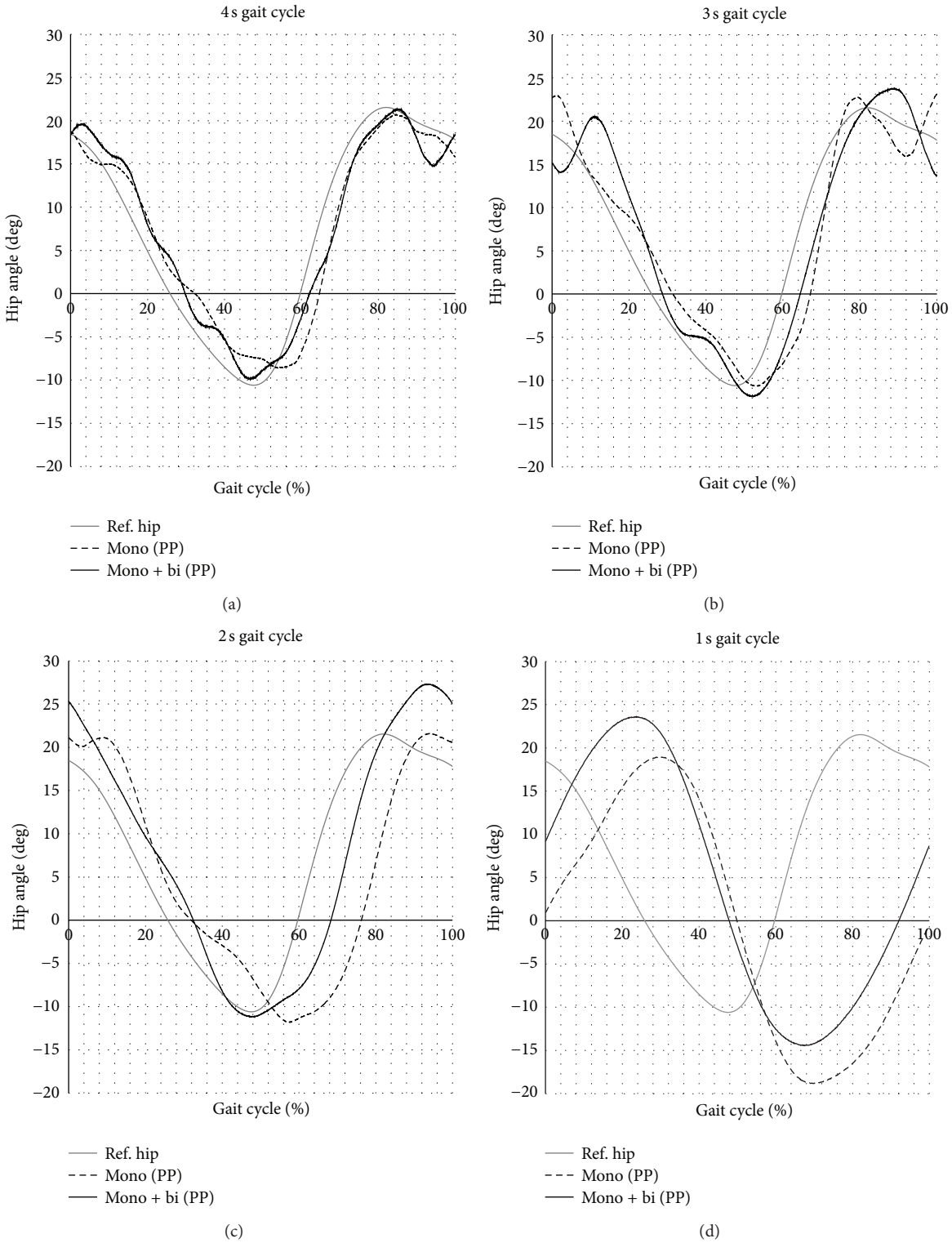

Figure 9: Hip joint trajectory for the control of the leg orthosis WO/S using a cocontraction model based PP controller.

in a more homogenously distributed way [18–20]. Even though the sources of the actuation system were different, the fundamental functions of these bi-articular actuators (PMA) should be similar. With a stable force assisting the movement of the leg orthosis, it reduces the coarse movement and improves the joints when compared to the leg orthosis actuated by the mono-articular actuators alone. The movement of the antagonistic bi-articular actuators was able to balance the coarse movement of the antagonistic mono-articular actuators at the joints, thus reducing the effect of the

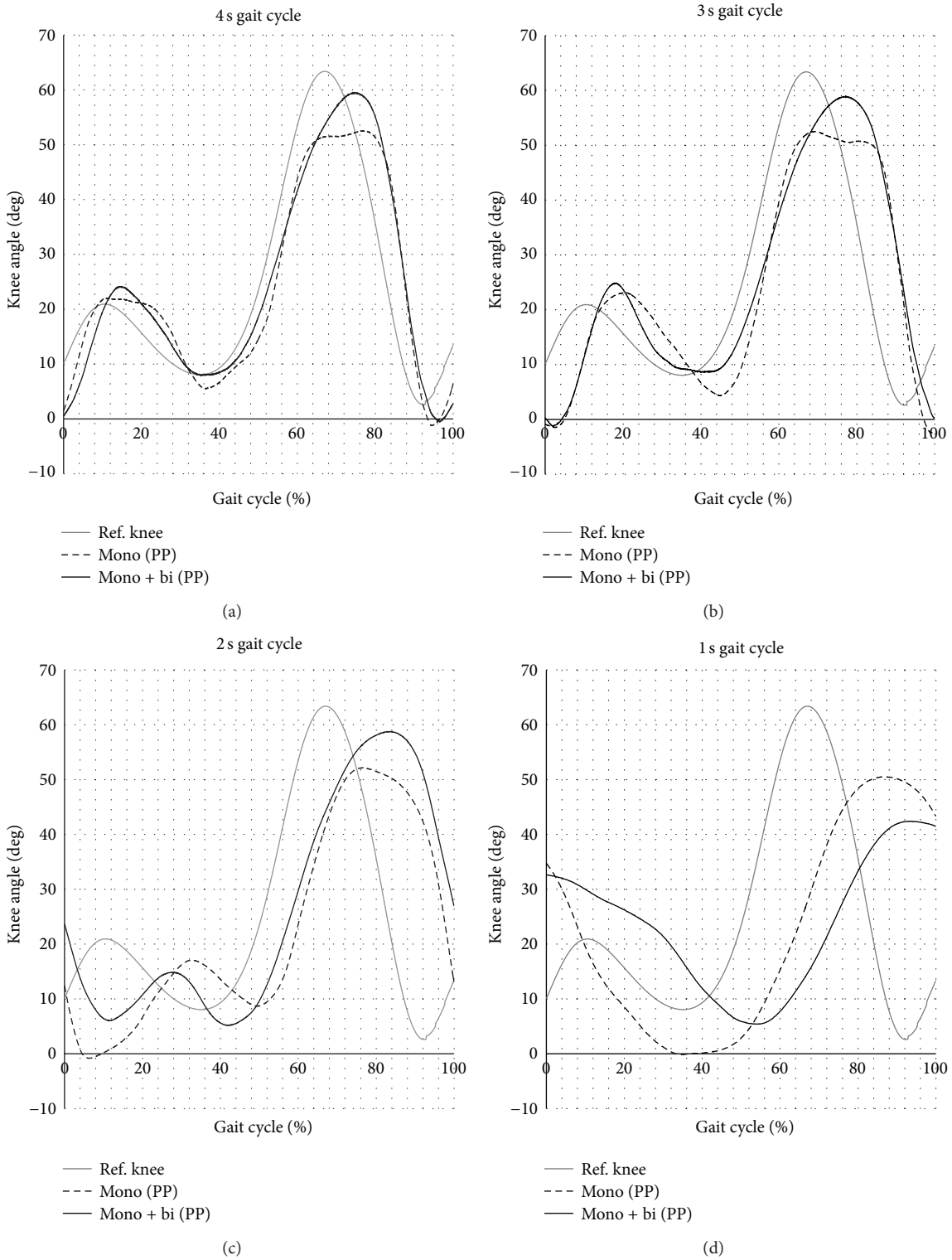

Figure 10: Knee joint trajectory for the control of the leg orthosis WO/S using a cocontraction model based PP controller.

hysteresis which was significant when implementing the mono-articular actuators alone WO/S. This is also due to the fact that the contraction of the PMA is in accordance with the hysteresis model. However, as the expansion of the PMA did not follow that of the hysteresis model, the co-contractive movements between the antagonistic mono- and bi-articular actuators were realized. At the GC speed of 1 second, the orthosis was not able to perform the gait motion completely with the heel strike stance. However, it was still able to demonstrate the "foot flat up to swing stance"

Table 3: Pearson coefficient of determination (r^2) for mono-articular (alone) and with addition of bi-articular actuators.

Joint actuators	Pearson coefficient of determination (r^2) for monoarticular and Biarticular actuators							
	Hip angle CC value				Knee angle CC value			
	4 s GC	3 s GC	2 s GC	1 s GC	4 s GC	3 s GC	2 s GC	1 s GC
Monoarticular actuators	0.8834	0.7921	0.3969	0.25	0.7569	0.4761	0.1764	0.0225
Mono- and Biarticular actuators	0.9025	0.8281	0.7744	0.0576	0.7569	0.49	0.1444	0.1296

Table 4: Pearson coefficient of determination (r^2) for co-contraction model based P and PP controllers.

Cocontraction model based	Pearson coefficient of determination (r^2) for P and PP Controllers							
	Hip angle CC value				Knee angle CC value			
	4 s GC	3 s GC	2 s GC	1 s GC	4 s GC	3 s GC	2 s GC	1 s GC
P controller	0.9139	0.7921	0.4761	0.0196	0.6241	0.4356	0.09	0.1444
PP controller	0.9274	0.8649	0.7744	0.0625	0.7744	0.5184	0.16	0.1681

which provides the feel of a gait motion. By implementing the derived cocontraction model, all the six antagonistic mono- and bi-articular actuators were able to operate simultaneously and co-contractively. Table 3 shows the Pearson coefficient of determination (r^2) for the first assessment where the control tests with mono-articular actuators (hip and knee joints) alone and with addition of bi-articular actuators WO/S were evaluated. This r^2 value indicates how well the data fits the reference joints' trajectory. The result shows that the addition of the bi-articular actuators produce much higher r^2 coefficient values at most GC speeds as compared to mono-articular actuators alone.

5.2. Control of the Leg Orthosis WO/S: Evaluation of Designed Controller Schemes. The focus in this second assessment is on the evaluation of the designed controller schemes and strategy. It was conducted to determine the limitations of the position-based controller when acting on its own, and the superiority of the combined position-pressure-based controller. Two experiments were conducted. In the first, the cocontraction model based P controller scheme was tested WO/S, and in the second, the cocontraction model based PP controller scheme was tested WO/S. Both tests were performed with the presence of mono- and bi-articular actuators and evaluated at different GC speeds of 4 seconds, 3 seconds, 2 seconds, and 1 second. Five trials were performed for each GC speed, and each trial consisted of five cycles including the initial cycle position. Thus, a total of 25 GCs were obtained for each GC speed. The average GC for each GC speed was then determined and illustrated in a graph. Table 4 shows the Pearson coefficient of determination (r^2) for the second assessment where the control tests for P and PP controllers of leg orthosis with mono- and bi-articular actuators WO/S were evaluated. The result shows that the addition of the pressure controller (PP) produces much higher r^2 coefficient values at all GC speeds as compared to position controller alone (P).

Figure 11 shows the trajectory evaluation of the joints of the leg orthosis controls between two designed controller schemes (i.e., cocontraction model based P controller and cocontraction model based PP controller) tested WO/S. From the results, it is evident that both designed controller schemes were able to wholly achieve the gait motion smoothly up to a GC speed of 2 seconds. However, failure to perform a complete gait motion was experienced at a higher GC speed of 1 second. These results reveal that PMA muscle activities (i.e., contraction, expansion, and response time) were curtailed at a GC speed above 2 seconds as the time allocated for completing the GC was drastically reduced. However, the results illustrate that the time response of the PMA muscle activity was much better with the implementation of the PP controller scheme compared to only the P controller scheme. Furthermore, the PP controller scheme was able to maintain the maximum angle extension achieved at the posterior side of the hip joint trajectory for all GC speeds compared to the P controller scheme (reduced with increase in GC speed) as can be seen in Figures 11(a) and 11(b) of hip joint trajectories. PMA control was insufficient with the P controller scheme alone as the dynamic characteristics of PMA include pressure activity. Through the introduction of a cocontraction model based PP controller scheme with modified design architecture, the maximum angle extension and time response of the system were improved at most GC speeds. This indicates that the addition of the pressure controller was able to improve the response time of the system as the pressure increased exponentially with the contraction of PMA, consequently increasing the speed of PMA muscle activity during contraction mode.

Based on the results, the trajectory of the joints was slightly coarse at slower GC speeds (i.e., 4 seconds and 3 seconds), as unlike the extension of the joint, the leg orthosis goes against the gravitational effect during the flexion of the hip joint. However, this effect was reduced with an increase in GC speed at the cost of insignificant angle extension. Conversely, only slight effects were detected in the knee trajectory for both controller schemes as the high muscle moment was larger at the hip joint compared to the knee joint. When implementing the PP controller scheme, the maximum angle extension at the posterior side of the knee joint trajectory was slightly reduced with the improvement in PMA muscle activity response time. This is due to the maximum contraction achievable by each PMA (30% of its original length) which results in a limitation of orthosis movements. The speed of PMA muscle activity will reduce considerably with

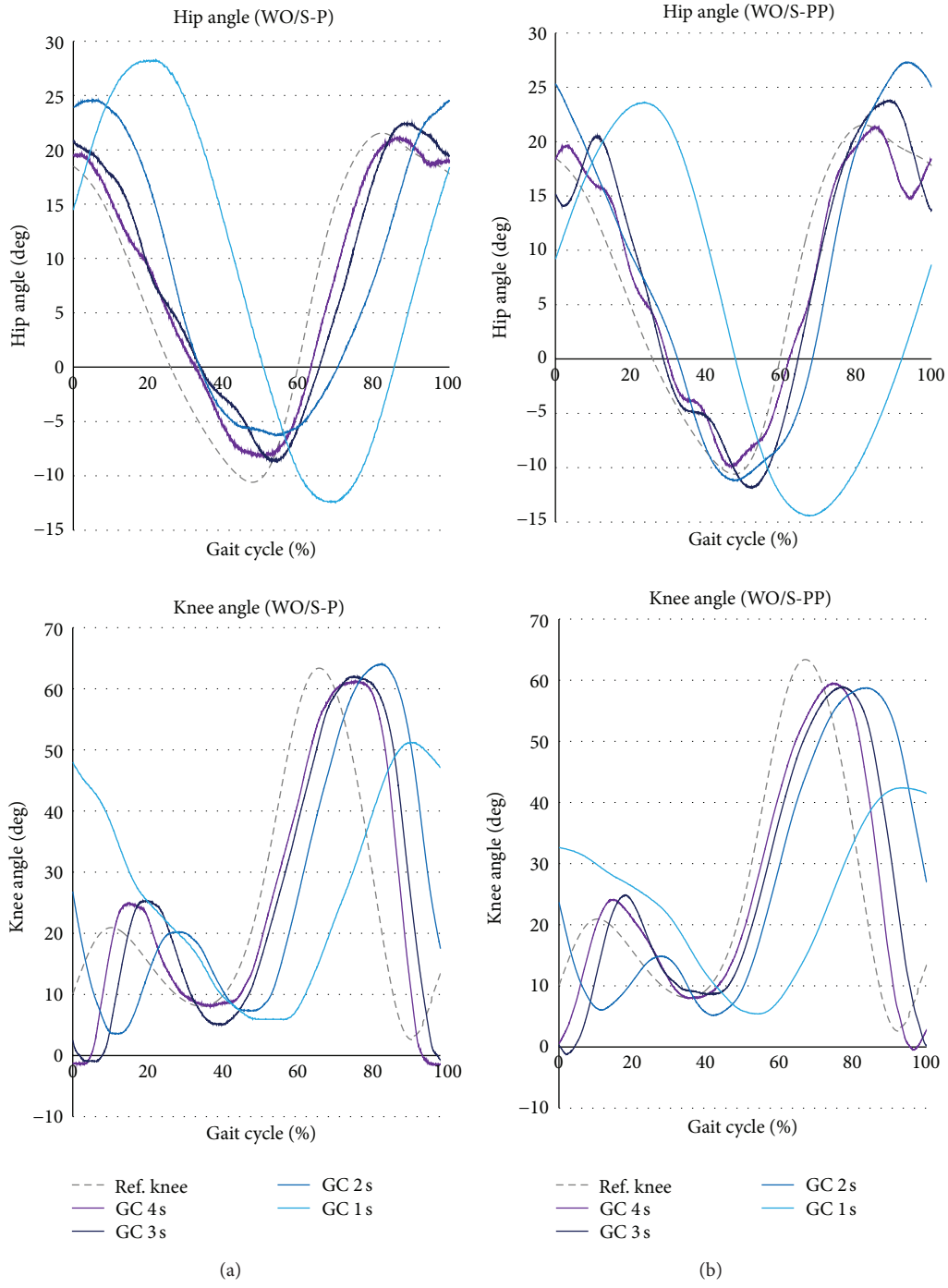

Figure 11: Hip and knee joints' trajectory evaluation of the leg orthosis controls between two designed controller schemes (i.e., P controller and PP controller) tested WO/S.

the approach of its maximum contraction. This affects the trajectory performance of the joints especially at the posterior side of the knee joint which requires a larger angle extension (63 degrees).

5.3. Control of the Leg Orthosis W/S. The focus in this third assessment is on the evaluation of the cocontraction model based P and PP controller scheme at the end point (EP) of the leg orthosis. It was conducted to determine the reliability of the designed controller scheme when implemented on leg orthosis and tested both WO/S and W/S. Two tests were conducted. The first involved leg orthosis controls WO/S and the second, leg orthosis W/S. Both tests were performed with the presence of mono- and bi-articular actuators. Similar to

previous assessments, the design controller scheme was evaluated at four GC speeds of 4 seconds, 3 seconds, 2 seconds, and 1 second. The normal GC speed of 1.25 seconds was not as necessary in the early stages of the gait rehabilitation therapy as it might not be able to furnish adequate afferent input to stimulate locomotor centres. However, during the later stages of rehabilitation therapy, gait training at the normal GC speed might be required. From the viewpoint of control architects, it is important to determine the system's maximum operating GC speed for the performance evaluation. A total of 25 GCs for each GC speed were collected, and the average GC was represented in a graph.

Figures 12 and 13 display the EP trajectory evaluation of the leg orthosis controls. This evaluation was carried out using the cocontraction model based P and PP controller scheme for tests WO/S and W/S. The results revealed that both designed controller schemes were able to achieve a good EP trajectory for all GC speeds of 4 seconds, 3 seconds, 2 seconds, and 1 second. Although the performance level dipped at a slower GC speed due to the inertia, good gait motion was displayed especially during the stance phase of GC both WO/S and W/S tests up to GC speed of 1 second. The coarse movement during the swing phase might be due to the increased load supported by the mono- and bi-articular actuators which forced the actuators into contraction mode to sustain the load much longer at a slower GC speed. This created an unbalanced state which disturbed the pressure activity of the antagonistic muscle actuators. Since the time allocated for completing one cycle was reduced with increases in GC speed, the posterior mono- and bi-articular actuators that contracted were unable to receive the control information fast enough to initiate the swing phase at the knee joint. This reduced the response time at the mid-swing phase (60~80% GC) due to the slowing down of PMA muscle activity as it approached maximum contraction.

To increase the response time of the design controller scheme at faster GC speeds, especially during the maximum angle extension of the knee joint, the constraints related to the actuator need to be reduced. These constraints include the inability of the system's operating pressure to withstand more than 5 (bars) of maximum load. The gravitational effect also affected the gait motion performance at the hip joint during the muscle flexion (0~50% GC) as the anterior mono-articular actuators and anterior bi-articular actuators were working against gravity during the leg expansion. This "leg expansion" is the gait motion from the heel strike stance up to toe off stance. It is an observed fact that the performance of the PMA controls faltered in the face of the gravitational effect. Therefore, it might be practical to lower the muscle activation level of the actuators in expansion mode so as to reduce the gravitational effect on the orthosis. Additionally, the effect can also be reduced by increasing the PMA muscle activity and the GC speed.

To determine the performance of the design controller schemes for both WO/S and W/S tests, the evaluation will be based on the effective work and the inertia produced by the EP trajectory of the leg orthosis controls. Figure 14 shows the effective work and inertia for the control of leg orthosis for both WO/S and W/S tests using cocontraction model based P and PP controllers. It is illustrated using mean value and standard deviation. Based on the researches carried out by Banala et al., to quantitatively determine the amount of adaptation, they implement a measure called "footpath deviation area." This area is the geometric area included between the swing phases of given foot trajectory and prescribed trajectory. The amount of area is the deviation of given trajectory from prescribed trajectory in the template [6, 7]. By using the same principle, the effective work is defined as the area covered by the EP trajectory within the reference trajectory (inside area), while inertia is defined as the area covered by the EP trajectory outside the reference trajectory (outside area). These data (i.e., effective work and inertia) were measured as ratio of the covered area to the total reference trajectory area. It is inevitable that the inertia will eventually occur as we tried to increase the GC speed from 4 s GC (0.35 m/s) up to 1 s GC (1.40 m/s), in which similar patterns can also be observed in [6]. Therefore, over 60% of effective work was judged as the minimum requirement to determine whether the leg orthosis was able or not to follow the reference foot trajectory. However, the total work done by the orthosis is defined as the sum of the effective work and inertia.

For the tests WO/S, both controller schemes produced nearly comparable effective work at the evaluated GC speeds of 4 seconds, 3 seconds, 2 seconds, and 1 second with 60% up to 89% of the ideal value. This effective work was reduced with the increases in the GC speed as the maximum knee angle extension achieved was reduced. However, with over 60% effective work achieved at all GC speeds; both designed controller schemes can be presumed to work properly. On the other hand, the inertia also occurred as the EP trajectory deviated outward from the reference trajectory. This inertia will always present at every GC speed due to the deviation. However, this inertia magnitude will vary with the increase of GC speed. Based on Figure 14(a), it can be seen that the cocontraction model based P controller was generating much higher inertia during the controls of leg orthosis with −13% up to −54% inertia as compared to −11% up to −43% inertia using cocontraction model based PP controller at all GC speeds. With these data, the leg orthosis was then tested W/S to determine the reliability of the designed controller schemes.

For the tests W/S, both controller schemes also produced nearly comparable effective work at the evaluated GC speeds of 4 seconds, 3 seconds, 2 seconds, and 1 second with 63% up to 85% of the ideal value. This effective work was maintained with over 60% effective work achieved at all GC speeds when compared to the test WO/S. On the other hand, based on the generated inertia evaluation, the inertia produced when using the cocontraction model based P controller was increasing with the increase of the GC speed, especially at the faster GC speeds of 2 seconds and 1 second. This indicates that the P controller alone was not enough to control the EP trajectory of the leg orthosis in the presence of inertia effect. However, when using the cocontraction model based PP controller, it was able to maintain the inertia produced at all evaluated GC speeds when tested both WO/S and W/S as illustrated in Figures 14(a) and 14(b). The generated inertia was around −13% up to −45% inertia (almost similar to the test WO/S with −11% up to −43% inertia) as compared to

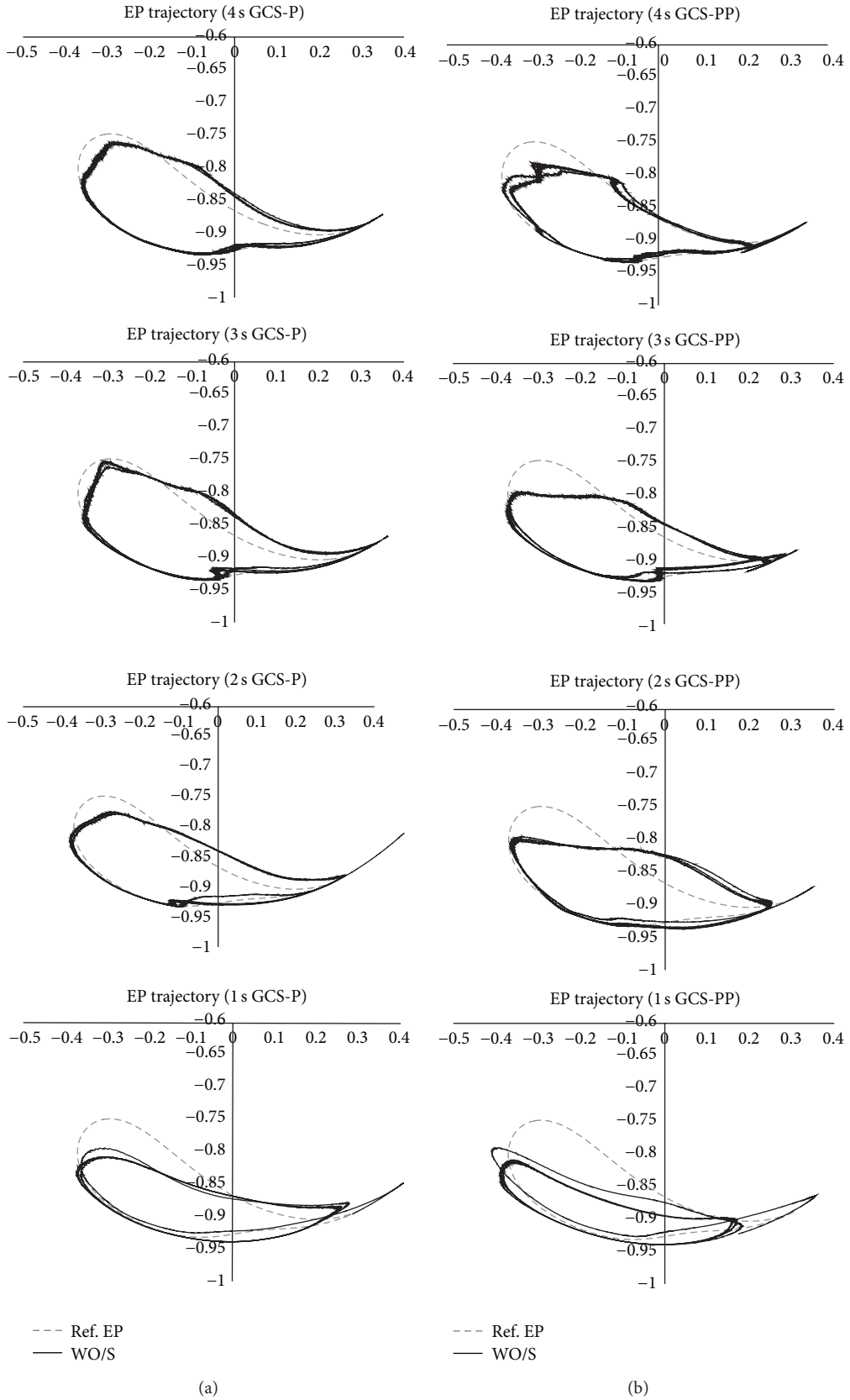

Figure 12: End point trajectory for the leg orthosis WO/S using cocontraction model based P and PP controllers.

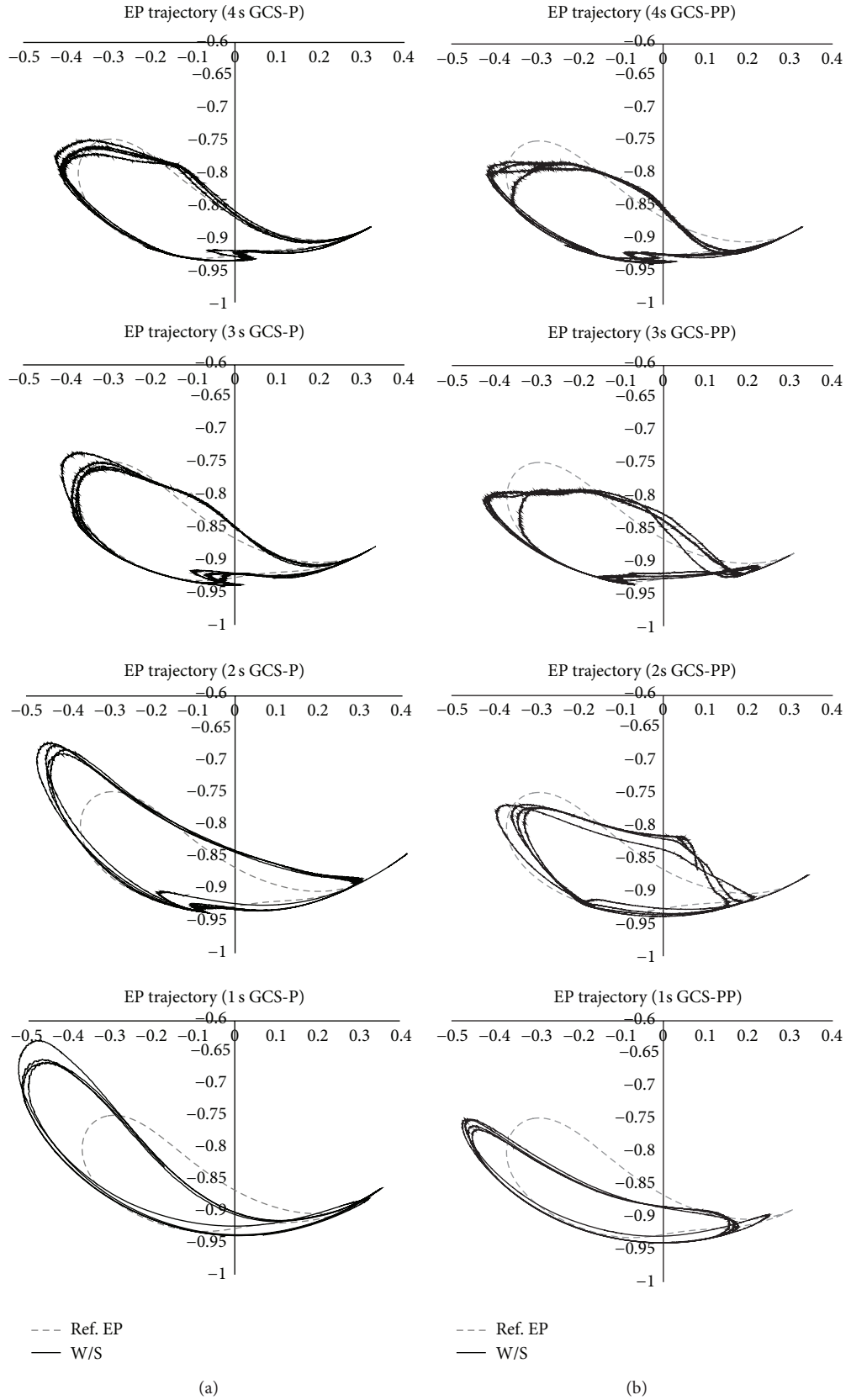

Figure 13: End point trajectory for the leg orthosis W/S using cocontraction model based P and PP controllers.

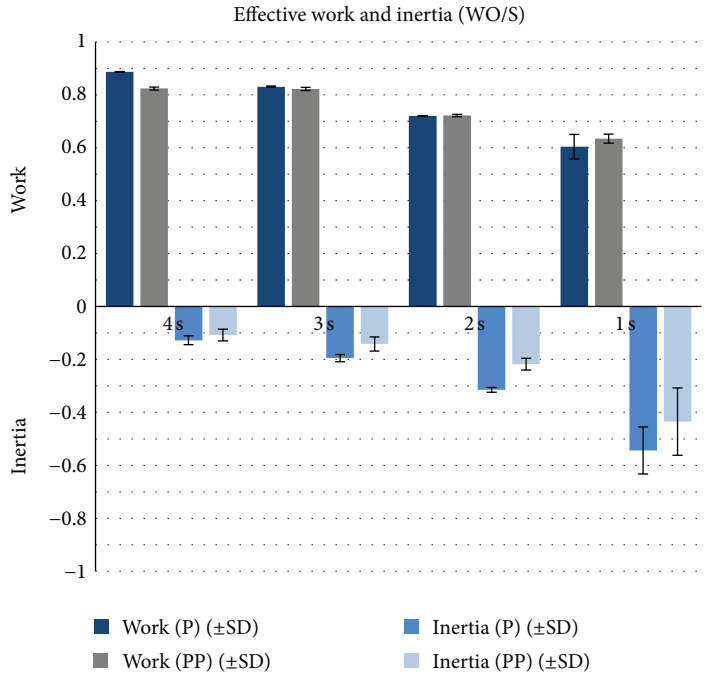

(a)

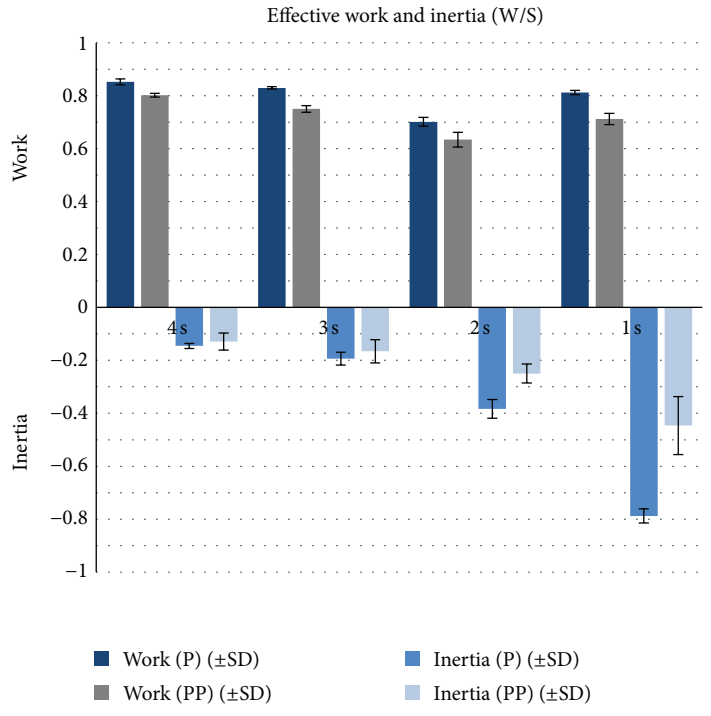

(b)

Figure 14: Effective work and inertia for the control of leg orthosis for both WO/S and W/S tests using cocontraction model based P and PP controllers.

−15% up to −79% inertia when using P based controller scheme. This concludes that the PP controller scheme was able to correspond to the inertia effect and thus gave a more stable EP trajectory of the leg orthosis at the evaluated GC speeds.

6. Conclusions

This research introduces the designed controller scheme and strategy to optimize the control of bi-articular actuators in co-contractive movements with the presence of mono-articular

actuators. The approach strategy for this designed controller scheme is the derivation of a cocontraction model which facilitates the implementation of position and pressure-based controllers. The proposed cocontraction model based PP controller scheme correlates information on the joints with the dynamic characteristics (i.e., contraction and pressure) of the PMA. Input patterns are then generated for the antagonistic mono- and bi-articular actuators compared to the other control algorithms for PMA that predict or measure the required torque for the joints.

Three tests were performed on the leg orthosis with the first using mono-articular actuators alone tested WO/S; the second with the addition of bi-articular actuators tested WO/S; and the third with the addition of bi-articular actuators tested W/S. Three assessments were evaluated to determine the performance of the designed controller scheme. The first assessment summarized that the addition of bi-articular actuators improved the joint stiffness of both the hip and knee. The bi-articular actuators also stabilized the coarse movements created by the mono-articular actuators during flexion of the joints and improved the maximum angle extension achieved at the knee joint. The second assessment concluded that compared to using the position based controller alone, the inclusion of the pressure-based controller improved the response time of PMA muscle activities due to the effects of contraction and expansion. The designed controller scheme was able to achieve complete gait motion of leg orthosis (i.e., hip and knee joints) until a GC speed of 2 seconds with a slight time shift of approximately only 0.2 seconds. The third assessment concluded that the cocontraction model based PP controller scheme was able to achieve a good EP trajectory of the leg orthosis up to GC speed of 1 second. The effective work achieved was over 60% of ideal value at all GC speeds of 4 seconds, 3 seconds, 2 seconds, and 1 second. Moreover, the generated inertia was also maintained at all GC speeds. This concludes that the PP controller scheme was able to correspond to the inertia effect and then optimize the controls of leg orthosis. The modified control scheme will be introduced in the next assessment to consider the gravitational effect on the antagonistic actuators as to improve control of the EP trajectory of the leg orthosis.

Conflict of Interests

The authors declare that they have no conflict of interests.

Acknowledgment

This work was supported by KAKENHI: Grant-in-Aid for Scientific Research (B) 21300202.

References

[1] G. Colombo, M. Wirz, and V. Dietz, "Driven gait orthosis for improvement of locomotor training in paraplegic patients," *Spinal Cord*, vol. 39, no. 5, pp. 252–255, 2001.

[2] S. Jezernik, G. Colombo, and M. Morari, "Automatic gait-pattern adaptation algorithms for rehabilitation with a 4-DOF robotic orthosis," *IEEE Transactions on Robotics and Automation*, vol. 20, no. 3, pp. 574–582, 2004.

[3] L. Lünenburger, G. Colombo, and R. Riener, "Biofeedback for robotic gait rehabilitation," *Journal of NeuroEngineering and Rehabilitation*, vol. 4, article 1, 2007.

[4] J. F. Veneman, R. Kruidhof, E. E. G. Hekman, R. Ekkelenkamp, E. H. F. Van Asseldonk, and H. Van Der Kooij, "Design and evaluation of the LOPES exoskeleton robot for interactive gait rehabilitation," *IEEE Transactions on Neural Systems and Rehabilitation Engineering*, vol. 15, no. 3, pp. 379–386, 2007.

[5] H. Vallery, J. Veneman, E. van Asseldonk, R. Ekkelenkamp, M. Buss, and H. van Der Kooij, "Compliant actuation of rehabilitation robots," *IEEE Robotics and Automation Magazine*, vol. 15, no. 3, pp. 60–69, 2008.

[6] S. K. Banala, S. H. Kim, S. K. Agrawal, and J. P. Scholz, "Robot assisted gait training with active leg exoskeleton (ALEX)," *IEEE Transactions on Neural Systems and Rehabilitation Engineering*, vol. 17, no. 1, pp. 2–8, 2009.

[7] S. K. Banala, S. K. Agrawal, S. H. Kim, and J. P. Scholz, "Novel gait adaptation and neuromotor training results using an active leg exoskeleton," *IEEE/ASME Transactions on Mechatronics*, vol. 15, no. 2, pp. 216–225, 2010.

[8] V. Monaco, G. Galardi, M. Coscia, D. Martelli, and S. Micera, "Design and evaluation of NEUROBike: a neuro-rehabilitative platform for bedridden post-strike patients," *IEEE Transactions on Neural Systems and Rehabilitation Engineering*, vol. 20, no. 6, 2012.

[9] D. J. Reinkensmeyer, D. Aoyagi, J. L. Emken et al., "Tools for understanding and optimizing robotic gait training," *Journal of Rehabilitation Research and Development*, vol. 43, no. 5, pp. 657–670, 2006.

[10] M. Pietrusinski, I. Cajigas, G. Severini, P. Bonato, and C. Mavroidis, "Robotic gait rehabilitation trainer," *IEEE/ASME Transactions on Mechatronics*, no. 99, pp. 1–10, 2013.

[11] A. Taherifar, M. Mousavi, A. Rassaf, F. Ghiasi, and M. R. Hadian, "LOKOIRAN—a novel robot for rehabilitation of spinal cord injury sand stroke patients," in *Proceedings of the RSI/ISM International Conference on Robotics and Mechatronics*, Tehran, Iran, 2013.

[12] S. Hussain, S. Q. Xie, and P. K. Jamwal, "Adaptive impedance control of a robotic orthosis for gait rehabilitation," *IEEE Transactions on Cybernetics*, vol. 43, no. 3, 2013.

[13] S. Hussain, S. Q. Xie, and P. K. Jamwal, "Robust nonlinear control of an intrinsically compliant robotic gait training orthosis," *IEEE Transactions on Systems, Man, and Cybernetics*, vol. 43, no. 3, 2013.

[14] Y. Shibata, S. Imai, T. Nobutomo, T. Miyoshi, and S.-I. Yamamoto, "Development of body weight support gait training system using antagonistic bi-articular muscle model," in *Proceedings of the 32nd Annual International Conference of the IEEE Engineering in Medicine and Biology Society (EMBC '10)*, pp. 4468–4471, Buenos Aires, Argentina, September 2010.

[15] S.-I. Yamamoto, Y. Shibata, S. Imai, T. Nobutomo, and T. Miyoshi, "Development of gait training system powered by pneumatic actuator like human musculoskeletal system," in *Proceedings of the IEEE International Conference on Rehabilitation Robotics (ICORR '11)*, Zurich, Switzerland, July 2011.

[16] M. Kumamoto, T. Oshima, and T. Fujikawa, "Control properties of a two-joint link mechanism equipped with mono- and bi-articular actuators," in *Proceedings of the 9th IEEE International Workshop on Robot and Human Interactive Communication (RO-MAN '00)*, pp. 400–404, Osaka, Japan, September 2000.

[17] S. Shimizu, N. Momose, T. Oshima, and K. Koyanagi, "Development of robot leg which provided with the bi-articular actuator for training techniques of rehabilitation," in *Proceedings of the 18th IEEE International Symposium on Robot and Human Interactive (RO-MAN '09)*, pp. 921–926, Toyama, Japan, October 2009.

[18] V. Salvucci, S. Oh, and Y. Hori, "Infinity norm approach for precise force control of manipulators driven by Bi-articular actuators," in *Proceedings of the 36th Annual Conference of the IEEE Industrial Electronics Society (IECON '10)*, pp. 1908–1913, November 2010.

[19] V. Salvucci, S. Oh, Y. Hori, and Y. Kimura, "Disturbance rejection improvement in non-redundant robot arms using bi-articular actuators," in *Proceedings of the IEEE International Symposium on Industrial Electronics (ISIE '11)*, pp. 2159–2164, June 2011.

[20] V. Salvucci, Y. Kimura, S. Oh, and Y. Hori, "Experimental verification of infinity norm approach for force maximization of manipulators driven by bi-articular actuators," in *Proceedings of the American Control Conference (ACC '11)*, pp. 4105–4110, San Francisco, Calif, USA, July 2011.

[21] M. A. Mat Dzahir, T. Nobutomo, and S. I. Yamamoto, "Development of body weight support gait training system using pneumatic McKibben actuators: control of lower extremity orthosis," in *Proceeding of the International Conference of the IEEE EMBS*, Osaka, Japan, 2013.

[22] M. Frey, G. Colombo, M. Vaglio, R. Bucher, M. Jörg, and R. Riener, "A novel mechatronic body weight support system," *IEEE Transactions on Neural Systems and Rehabilitation Engineering*, vol. 14, no. 3, pp. 311–321, 2006.

[23] H. J. A. van Hedel, L. Tomatis, and R. Müller, "Modulation of leg muscle activity and gait kinematics by walking speed and bodyweight unloading," *Gait and Posture*, vol. 24, no. 1, pp. 35–45, 2006.

[24] J. Von Zitzewitz, M. Bernhardt, and R. Riener, "A novel method for automatic treadmill speed adaptation," *IEEE Transactions on Neural Systems and Rehabilitation Engineering*, vol. 15, no. 3, pp. 401–409, 2007.

[25] B. Tondu and P. Lopez, "Modeling and control of McKibben artificial muscle robot actuators," *IEEE Control Systems Magazine*, vol. 20, no. 2, pp. 15–38, 2000.

[26] T. Miyoshi, K. Hiramatsu, S.-I. Yamamoto, K. Nakazawa, and M. Akai, "Robotic gait trainer in water: development of an underwater gait-training orthosis," *Disability and Rehabilitation*, vol. 30, no. 2, pp. 81–87, 2008.

[27] S. Balasubramanian, J. Ward, T. Sugar, and J. He, "Characterization of the dynamic properties of pneumatic muscle actuators," in *Proceedings of the IEEE 10th International Conference on Rehabilitation Robotics (ICORR '07)*, pp. 764–770, Noordwijk, The Netherlands, June 2007.

[28] J. Bae and M. Tomizuka, "A gait rehabilitation strategy inspired by an iterative learning algorithm," *Mechatronics*, vol. 22, no. 2, pp. 213–221, 2012.

[29] K. K. Ahn and D. C. T. Tu, "Improvement of the control performance of Pneumatic Artificial Muscle Manipulators using an intelligent switching control method," *KSME International Journal*, vol. 18, no. 8, pp. 1388–1400, 2004.

[30] T. D. C. Thanh and K. K. Ahn, "Nonlinear PID control to improve the control performance of 2 axes pneumatic artificial muscle manipulator using neural network," *Mechatronics*, vol. 16, no. 9, pp. 577–587, 2006.

[31] M. A. Mat Dzahir, T. Nobutomo, and S. I. Yamamoto, "Antagonistic mono- and bi-articular pneumatic muscle actuator control from gait training system using contraction model," in *Proceedings of the IEEE International Conference on Bio-Science and Bio-Robotics*, Rio de Janeiro, Brazil, 2013.

[32] D. A. Winter, *Winter, Biomechanics and Motor Control of Human Movement*, John Wiley & Sons, 4th edition, 2009.